CHALMERS

Dissolved Air Flotation

Numerical investigation of the contact zone on geometry, multiphase flow and needle valves

Master of Science Thesis in the Master's Programme Geo and Water Engineering

AREZOU BABAAHMADI

Department of Civil and Environmental Engineering
Division of Water and Environment Technology
CHALMERS UNIVERSITY OF TECHNOLOGY
Göteborg, Sweden 2010
Master's Thesis 2010:123

MASTER'S THESIS 2010:123

Dissolved Air Flotation

Numerical investigation of the contact zone on geometry, multiphase flow and needle valves

Master of Science Thesis in the Master's Programme Geo and Water Engineering

AREZOU BABAAHMADI

Department of Civil and Environmental Engineering
Division of Water and Environment Technology
CHALMERS UNIVERSITY OF TECHNOLOGY
Göteborg, Sweden 2010

Dissolved Air Flotation

Numerical investigation of the contact zone on geometry, multiphase flow and needle valves

Master of Science Thesis in the Master's Programme Geo and Water Engineering

AREZOU BABAAHMADI

Examensarbete / Institutionen för bygg- och miljöteknik,
Chalmers tekniska högskola 2010:123

Department of Civil and Environmental Engineering
Division of Water and Environment Technology
Chalmers University of Technology
SE-412 96 Göteborg
Sweden
Telephone: + 46 (0)31-772 1000

Printed by:

Department of Civil and Environmental Engineering
Göteborg, Sweden 2010

Dissolved Air Flotation

Numerical investigation of the contact zone on geometry, multiphase flow and needle valves

Master of Science Thesis in the Master's Programme Geo and Water Engineering

AREZOU BABAAHMADI
Department of Civil and Environmental Engineering
Division of Water and Environment Technology
Chalmers University of Technology

ABSTRACT

One of the well known intermediate stages to treat water and wastewater is Dissolved Air Flotation (DAF). In order to design an efficient DAF unit, it is important to study the system and get familiar with the flow structure in it. Computational Fluid Dynamics (CFD) is used as a tool to study a flotation unit.

Most of the previous CFD studies of DAF have been set up in two dimensions in order to reduce the required computational time and space. By modeling only in two dimensions the effects of the flow from the needle valves is excluded. This study aims to consider these effects through three-dimensional modeling. The aim is to study the contact zone considering variables affecting this part of the DAF unit. These variables are number of needle valves, tank geometry, side wall effects and presence of the separation zone.

In this study two- and three-dimensional representations of the tank are evaluated. Simulations account for both one-phase and two-phase flow and the flow is assumed to be in steady state. The geometry of the tank is modeled in GAMBIT and exported to FLUENT 12 to perform the flow simulations. The flow in the tank is assumed to be turbulent, which is modeled with the standard and the realizable k-ε models. Standard wall function and non equilibrium wall functions are used for these models respectively. The Lagrangian model is used to simulate the two-phase flow consisting of air bubbles and water. Validation of the results is made by comparing the simulated flow with previously measured flow patterns in a pilot DAF tank.

Results show that convergence is very connected to the outlet location and the further away the outlet is located from the contact zone the easier it is to reach a converged solution. The number of needle valves included in the model and the inclusion of the side walls are parameters found to have an effect on the flow structure in contact zone. The two-phase flow result predicts a movement of air bubbles toward the inlet zone a phenomenon not observed in the experimental measurements.

Key Words: Dissolved Air Flotation (DAF), Computational Fluid Dynamics (CFD), one phase flow, multiphase flow, turbulence

Contents

Preface

In this study Dissolved Air Flotation is modelled and flow structure in this tank is simulated by ANSYS FLUENT 12. The work is carried out from February 2010 to August 2010 at the department of Civil and Environmental Engineering.

This research study is done by Arezou BabaAhmadi as a researcher, Mia Bondelind and Assistant Professor Thomas Pettersson as supervisors.

I would like to thank my supervisors Mia Bondelind and Assistant Professor Thomas Pettersson, who supported me during this work.

I would also like to thank Måns Lundh because of letting me use experimental data concluded from his work.

Göteborg, August 2010

Arezou BabaAhmadi

Notations

k	Turbulence Kinetic energy
Q_{in}	Inlet flow
Q_{out}	Outlet flow
Q_{rec}	Recycle flow
U	Velocity in x direction
V	Velocity in y direction
W	Velocity in z direction
α	Relaxation factor
ε	Energy dissipation rate
μ	Viscosity
ϑ	Kinematic viscosity
ρ	Density of water
ADV	Acoustic Doppler Velocimeter
CFD	Computational Fluid Dynamics
DAF	Dissolved Air Flotation
LDV	Laser Doppler Velocimeter
PIV	Particle Image Measurement

1 Introduction

The supply of fresh water and the treatment of wastewater is a very important issue addressed all around the world. There are many processes developed in order to treat water and wastewater, but how can we study these systems and improve them in a way that the efficiency increases? In order to answer this question the system has to be modelled in a simple way. With a model the systems sensitivity to different variables involved in the process can be evaluated. The water treatment processes can be described as all the activities used to improve the water quality for the end user. In this study, the aim is to model one part of the treatment process called Dissolved Air Flotation (DAF). With the model the flow structure inside the tank can be evaluated.

1.1 Objectives

It is difficult to evaluate what effects needle valves have on the flow structure in a DAF unit with a two-dimensional Computational Fluid Dynamic (CFD) model. Previous modelling has indicated that the representation of the needle valves in a numerical model can effect the flow structure in the contact zone, especially in a two-dimensional model. This study was instigated to evaluate the influence of the flow from the needle valves and to investigate different possibilities to numerically study only the contact zone of a DAF unit. The main aim of this master thesis was to examine different approaches to numerical studies of the flow in the contact zone in a Dissolved Air Flotation tank. The influence on the flow by several parameters was examined. These variables can be categorized as; needle valve characteristics, wall effects, outlet geometry and effects of including the separation zone. ANSYS FLUENT 12 is used as CFD code in this study.

1.2 Limitations

The complexity of the flow in a flotation tank, when accounting for both turbulence and the multiphase flow, requires long computational time and large memory, especially when studying the complete unit. Consequently, the modelled geometry will be limited and the full tank will not be modelled. Only one- and two-phase simulations are included in the study, i.e. the influence of the particles is not addressed in this work.

Moreover, tank geometry is modelled based on a down scale flotation unit that has been studied previously (Lundh, 2000). By modelling the same geometry it is possible to validate the numerical simulations and to compare them with the experimental measurements.

2 Background

A general description of a water treatment process is first presented in this chapter and thereafter a more detailed explanation of the Dissolved Air Flotation process will follow. A brief introduction to fluid dynamics will be provided with a review of previous modelling done in this field.

2.1 Water Treatment Process

Treatment plants producing potable water, used by industries and households, have to meet with chemical and microbiological standards set up by the World Health Organization (Viessman, 2005). Selections of treatment processes that are needed to meet up with the standards are very much dependent on the raw water quality. Generally, treatment plant processes can be divided in to three stages, Figure 1. The first stage includes pre-treatment, which is basically separation of coarse particles from the water using screening units and pre-sedimentation tanks. In the intermediate stage, known as coagulation-flocculation, chemicals known as coagulants like alum or polymers are added in order to coagulate fine particles. The flocculated particles are then called flocs. The flocs are removed by Dissolved Air Flotation, sedimentation and filtration units. The disinfection process is considered as the final stage to reach the chemical and microbiological standards.

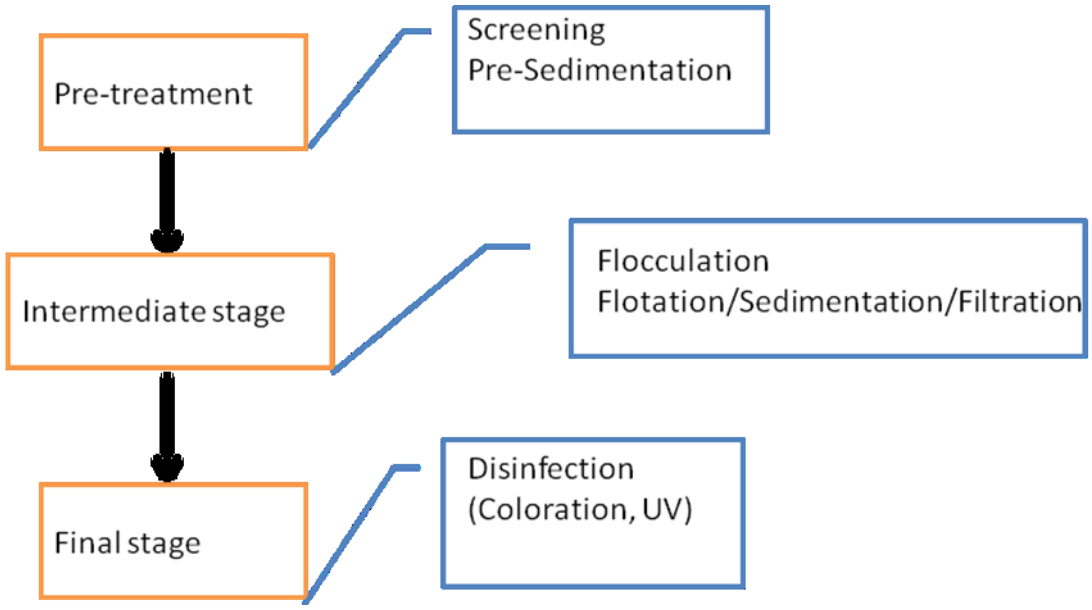

Figure 1. A general treatment process consists of three different stages. At the pre-treatment step coarse particles will be removed. At the intermediate stage, particles are coagulated and removed through sedimentation, flotation or filtration. At the final stage coloration or UV techniques will disinfect the water.

2.2 Flotation and Dissolved Air Flotation

The scope of this thesis is to numerically investigate the treatment process Dissolved Air Flotation (DAF) and therefore a more detailed description of the flotation process is presented in this part of the report.

In general, the idea behind flotation theory is that solid or liquid particles can be removed from a liquid phase by introducing them to fine air gas bubbles. The air

bubbles will attach to the flocs creating agglomerates. Having lower density than water, the agglomerates will rise up to the surface where they can be removed.

The flotation tank consists of three main zones called the inlet zone, the contact zone and the separation zone, Figure 2. The zones are separated from each other by baffle walls. The inlet zone is where pre-treated water enters the flotation tank. Through the needle valves air bubbles are added to the flow by injecting water saturated with air under high pressure into the contact zone. The contact zone is where the air bubbles are added to the flow creating a multiphase flow and basically this zone experiences a turbulent flow. The formed agglomerates will rise to the surface forming a foam layer in the separation zone and the treated water will move down toward the DAF outlet (Tchobanoglous, 2003). Advantages of using this method are superior removal of algae, improvement in water color and odor as well as possibility of having higher loading rates (Hague, 2001).

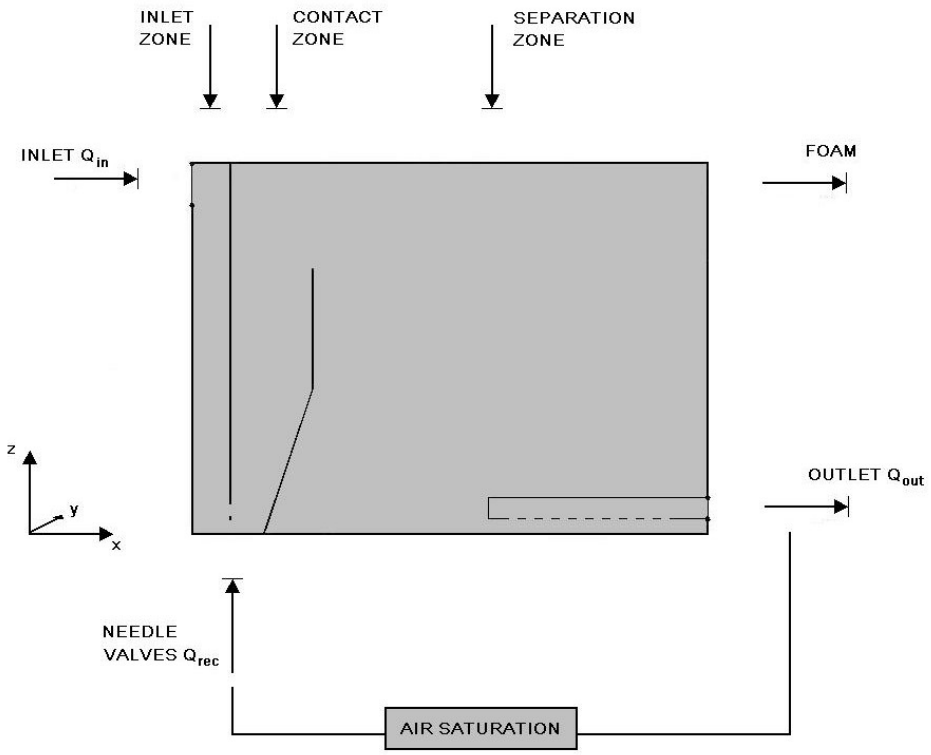

Figure 2. A schematic description of a Dissolved Air Flotation tank (Bondelind, 2009). Baffle walls divides the tank into the inlet zone, the contact zone and the separation zone. A portion of water collected at the outlet is recycled and saturated with air. It is then injected into the tank through the needle valves. Air bubbles will attach to the particles and bring the particles to the water surface where they are removed.

2.3 Similar projects

Although Computational Fluid Dynamics (CFD) analyses of Dissolved Air Flotation systems could be very beneficial, not many CFD studies regarding DAF units can be found in literature. Moreover, even fewer studies can be found that addresses the modelling of the contact zone. In this part of the report previous studies found in literature is presented briefly.

Hague (2001) used CFD to study a two-phase flow in a three-dimensional tank. The results in flotation zone were validated against both LDV and PIV measurements.

However except simulating flow pattern no analysis on the affects of different variables affecting flow structure in a DAF tank has been studied. A more recent study of a DAF unit have been presented by Emmanouil et al. (2007) who have modelled the two-phase flow in a two-dimensional geometry. The main aim in their study was to evaluate a malfunctioning DAF tank producing macro bubbles. In the study by Emmanouil et al. (2007) the best location to inject the air bubbles in their numerical model was investigated. The study presented by Emmanouil et al. (2007), has not been validated against experimental data. A two-dimensional model representing both the contact zone and the separation zone has been investigated by Fawcett (1997) with the aim of finding important DAF design parameters. With the two-dimensional model effects of the side walls could not be accounted for.

Moreover, Ta et al. (2001) have modelled the multiphase flow in both contact zone and separation zone and validated the results using ADV measurements. Considering complexities involved in multiphase flow simulations results could just be confirmed qualitatively. Guimet et al. (2007) have also studied DAF units. Their study shows agreement with experimental measurements done by Lundh (2000). However, very low injection rate from air nozzles has been considered in this simulation. Crossley and Rokjer (1999) made a CFD model of a DAF unit which was basically representing the separation zone. Results lack validation in this study. Also a thin strip of the whole tank have been modelled by Ta and Brignal (1997), which is a very good idea to reduce the computational time and space needed to model the whole tank in three dimensions.

2.4 Fluid Dynamics

The study of non static fluids is called fluid dynamics and the aim of it is to describe the properties of the fluid at a specific position in time. These properties can be categorized as velocity field, pressure, density and temperature (White, 2003). The general equations used to describe the flow are the Navier-Stokes equations and the continuity equation (Davidson, 1997).

$$\frac{\partial U}{\partial t} + U\frac{\partial}{\partial x}(U) + V\frac{\partial}{\partial y}(U) + W\frac{\partial}{\partial z}(U) = -\frac{1}{\rho}\frac{\partial P}{\partial x} + \vartheta\left(\frac{\partial^2 U}{\partial x^2} + \frac{\partial^2 U}{\partial y^2} + \frac{\partial^2 U}{\partial z^2}\right) \quad (2.1)$$

$$\frac{\partial V}{\partial t} + U\frac{\partial}{\partial x}(V) + V\frac{\partial}{\partial y}(V) + W\frac{\partial}{\partial z}(V) = -\frac{1}{\rho}\frac{\partial P}{\partial y} + \vartheta\left(\frac{\partial^2 V}{\partial x^2} + \frac{\partial^2 V}{\partial y^2} + \frac{\partial^2 V}{\partial z^2}\right)$$

$$\frac{\partial W}{\partial t} + U\frac{\partial}{\partial x}(W) + V\frac{\partial}{\partial y}(W) + W\frac{\partial}{\partial z}(W) = -\frac{1}{\rho}\frac{\partial P}{\partial z} + \vartheta\left(\frac{\partial^2 W}{\partial x^2} + \frac{\partial^2 W}{\partial y^2} + \frac{\partial^2 W}{\partial z^2}\right)$$

Where P is the pressure, U, V and W are velocities in x, y and z directions, ϑ is the kinematic viscosity. Usually continuity equation is included in Navier-Stokes equations, which can be written as

$$\frac{\partial \rho}{\partial t} + \frac{\partial \rho U}{\partial x} + \frac{\partial \rho V}{\partial y} + \frac{\partial \rho W}{\partial z} = 0 \quad (2.2)$$

2.4.1 Turbulent Flow

When the flow is irregular, diffusive, dissipative and changing stochastically, it is called turbulent. When having this situation, the fluid properties cannot be treated in the same way as in a laminar flow. By making the assumption that the fluid properties can be described by a mean value and a fluctuating part, turbulence can be accounted for. This changes the differential equations and an extra part will be added to the Navier-Stokes equations. Transport equations of one or two turbulent quantities, like kinetic energy (k) or its dissipation rate (ε), are derived and leads to the set of equations called k-ε equations (Davidson, 1997).

2.4.2 Multiphase Flow

With the addition of air bubbles to the flow field the flow is no longer a single phase flow, but consists of two phases: water and air bubbles. This is referred to as a multiphase flow. In Fluent there are two approaches available to solve the multiphase flow, either the Euler-Euler or the Euler-Lagrange approach. In this study the Euler-Lagrange method is chosen since the results can be later compared to the analysis done previously (Bondelind, 2009). In the Euler-Lagrange approach the fluid (water) is solved as a continuum, while the second phase (air) is solved as a large number of bubbles tracked in this calculated flow field (Fluent, 2006).

2.5 Computational Fluid Dynamics (CFD)

Finding a numerical solution of the differential equations governing mass transfer, momentum and energy for dynamic fluids, is the basic idea behind CFD analysis. The domain of interest is divided in to mesh cells. There is a measure point or a node within each cell, which is representative of the entire area within it. Boundary conditions have to be defined to solve the flow.

As unknown parameters will be estimated based on few known values, there is large amount of error at the beginning of calculations, which can be reduced by iterative solvers. As iterative solvers require computational space and time, computer programs should be used instead of hand calculations.

2.6 Validation methods

Previous experimental measurements of the flow field in a pilot DAF tank, (Lundh, 2000; Lundh 2002), are used to validate the numerical results. The measurement technique that was used in the pilot tank was Acoustic Doppler Velocimeter (ADV). Several cases with different measurement conditions were performed in the study by Lundh (2000, 2002). The cases used for validation in this study are named: M1, M3 and M4. The case M1 represents measurements made in the contact zone with one-phase flow and with the flow from the needle valves turned off. The case M3 is preformed with the same conditions as M1 with the only difference that the flow from the needle valves was turned on i.e. a flow of water without air bubbles is injected from the needle valves. The M4 case represents the two-phase flow measurements, where both air and water are injected from the needle valves. Due to the probe orientation during the measurements, case M1 tends to have larger errors than the other two cases. It was also observed that the air bubbles interfered with the probe when performing the velocity measurements reducing the magnitude of the velocities (Lundh, 2000). Therefore, the numerical simulations will only be compared qualitatively with the experimental measurements.

3 Method

The evaluation of how to model the contact zone is carried out by examining different geometries of the entity. The geometry is set up in the software GAMBIT 2.3.16 and the model is thereafter exported to FLUENT 12, where the flow pattern and air distribution are simulated. In order to validate the results, the geometry of the numerical model of the tank is matched with a pilot tank used by Lundh (2000) see Table 1. For all numerical models the inlet is modelled as being distributed in the width direction and set as a velocity inlet. The water surface is modelled as a frictionless wall and the outlet is modelled as a pressure outlet. Two-phase flow simulations are carried out for the two- and three-dimensional models with one needle valve and also for the thin strip of the whole tank.

Three different representations of the contact zone have been evaluated:

- A two-dimensional representation of the inlet and contact zone, which is called model A.
- A three-dimensional representation of the inlet and contact zone, which is called model B and C.
- A three-dimensional representation of complete tank including the inlet, contact zone and separation zone, which is called model D.

Each of the models A, B and C are divided in to two models, which differ regarding their outlet geometry. Models A_1, B_1 and C_1 have an outlet at the top of the contact zone, Figure 3. Models A_2, B_2, and C_2, Figure 4, 5 and 6, respectively, have an extended outlet, which is designed due to difficulties with finding a converged solution with previous models.

Two-dimensional model

In the two-dimensional models, Figure 3 (first one from the left) and Figure 4, the needle valves are modelled as a single point injection. As a result during one-phase flow analysis it is not possible to account for effects of water injection from needle valves.

Three-dimensional model

In all three-dimensional models, the needle valves are modelled as a rectangular box. The flow pattern in the tank is simulated with the flow from the needle valves turned either off or on. The side walls are modelled as symmetric walls.

Model B_1 and B_2, Figure 3 (middle figure) and Figure 5, represent one third of the tank width, as shown in Figure 8. Here only one needle valve is considered. Effects on the flow pattern when including a third dimension is examined by comparing model A and B.

The three-dimensional models C_1 and C_2, Figure 3 (third figure from the left) and Figure 6, show two thirds of the tank width, Figure 8, and two needle valves are included in this model. Effects of the number of needle valves on the flow pattern are examined through comparison between model C and B results.

The three-dimensional model D, Figure 7, referred to as the thin strip, models one third (in width) of the complete tank. Effects of the separation zone on the flow pattern in the contact zone are studied through this model.

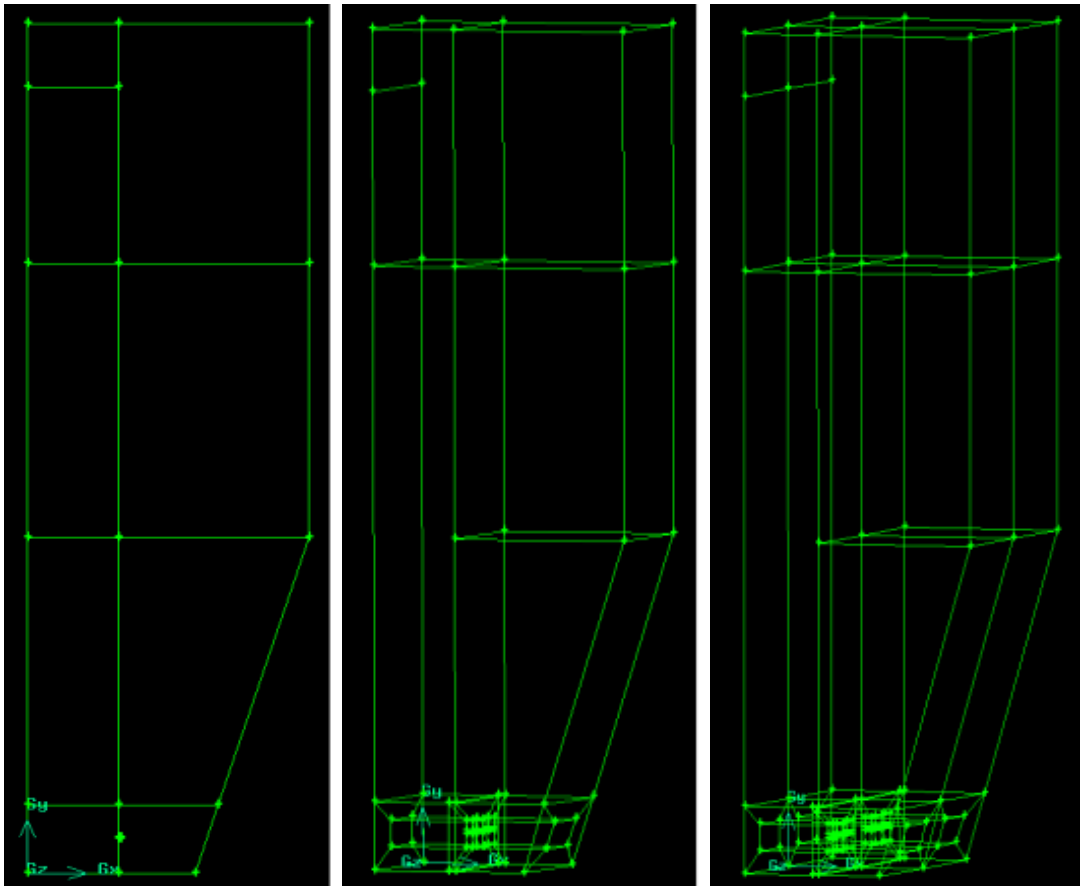

Figure 3. A schematic description of the two- and three-dimensional models of the inlet and the contact zone constructed in GAMBIT. From left to right model A_1, B_1 and C_1. One needle valve is included in model B_1 and two needle valves are included in model C_1.

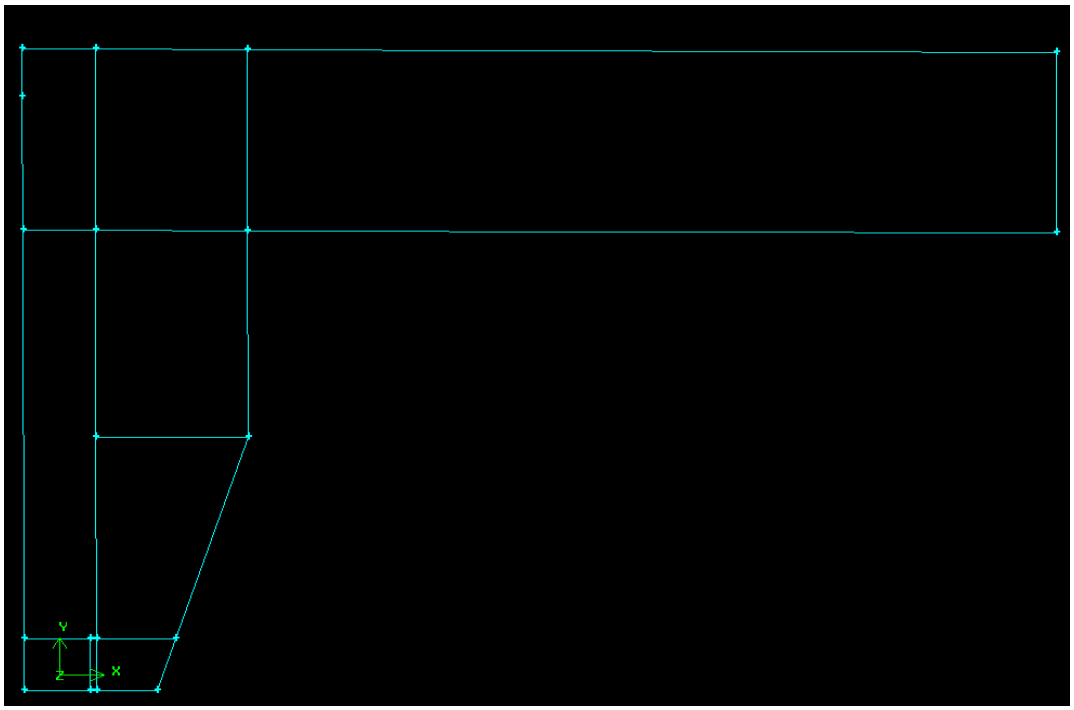

Figure 4. A schematic representation of the two-dimensional model A_2 with an extended outlet geometry.

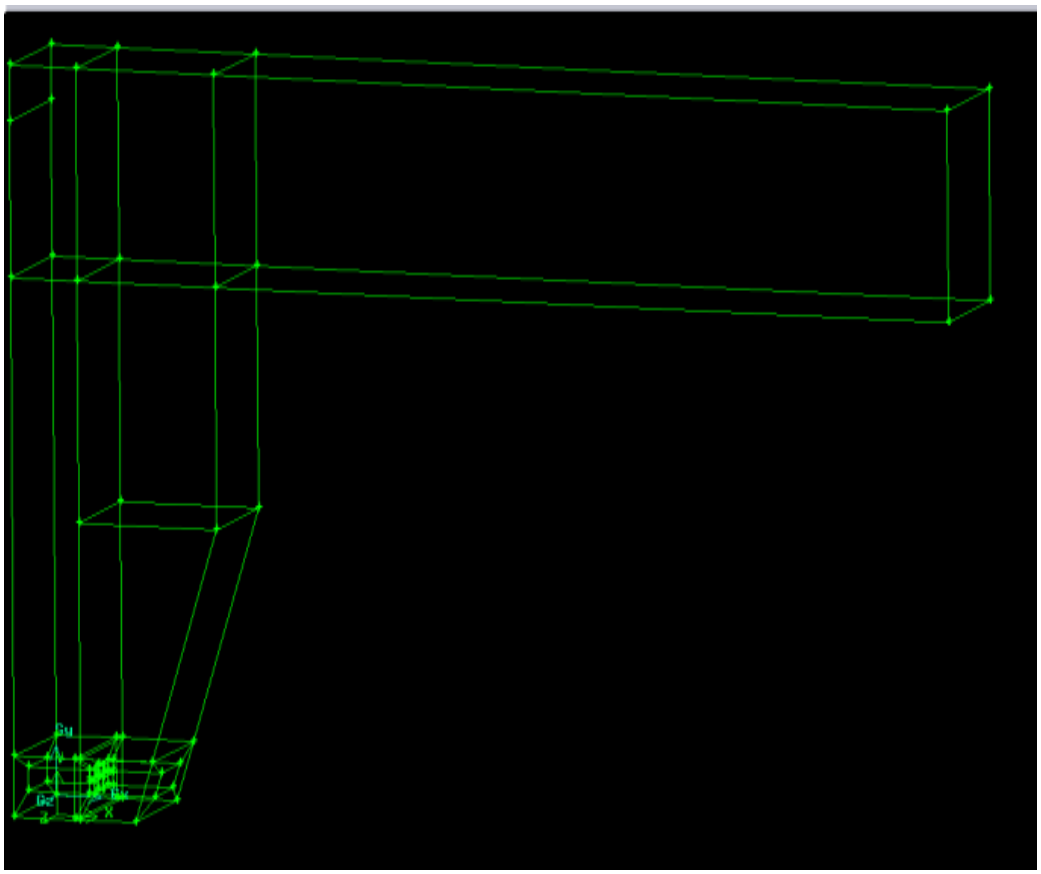

Figure 5. A schematic description of the three-dimensional B_2 model with an extended outlet geometry. One needle valve is modelled in the geometry.

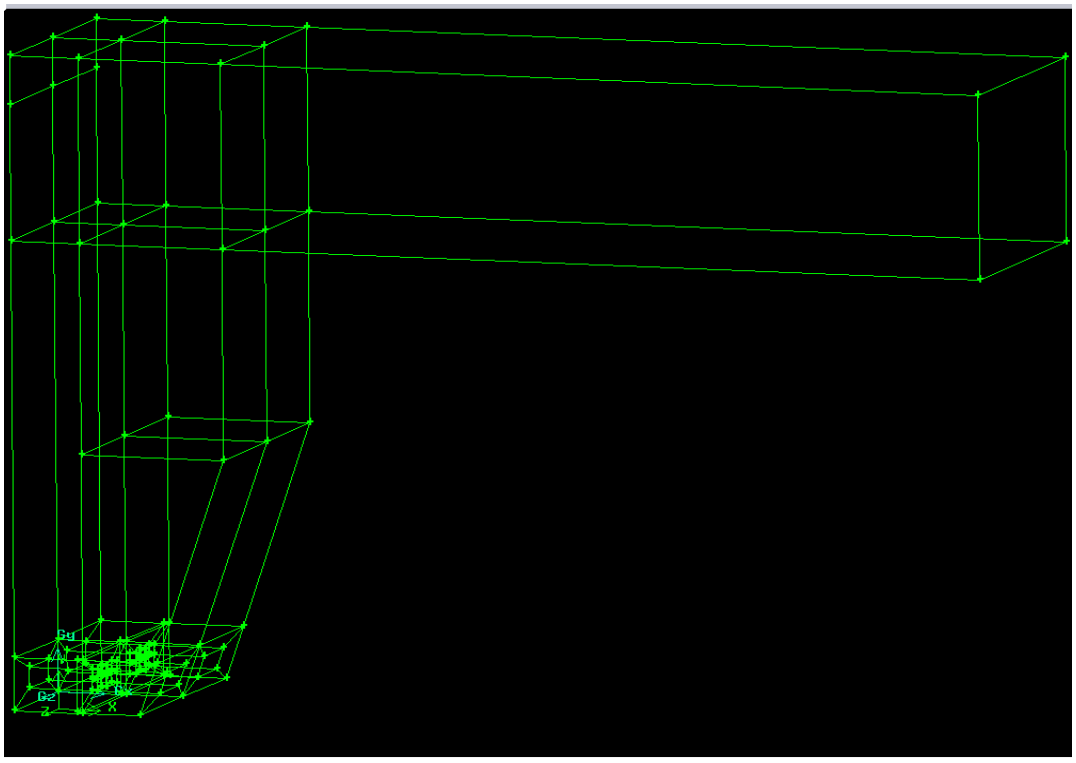

Figure 6. A schematic description of the three-dimensional C_2 model with an extended outlet geometry. Two needle valves are modelled in the geometry.

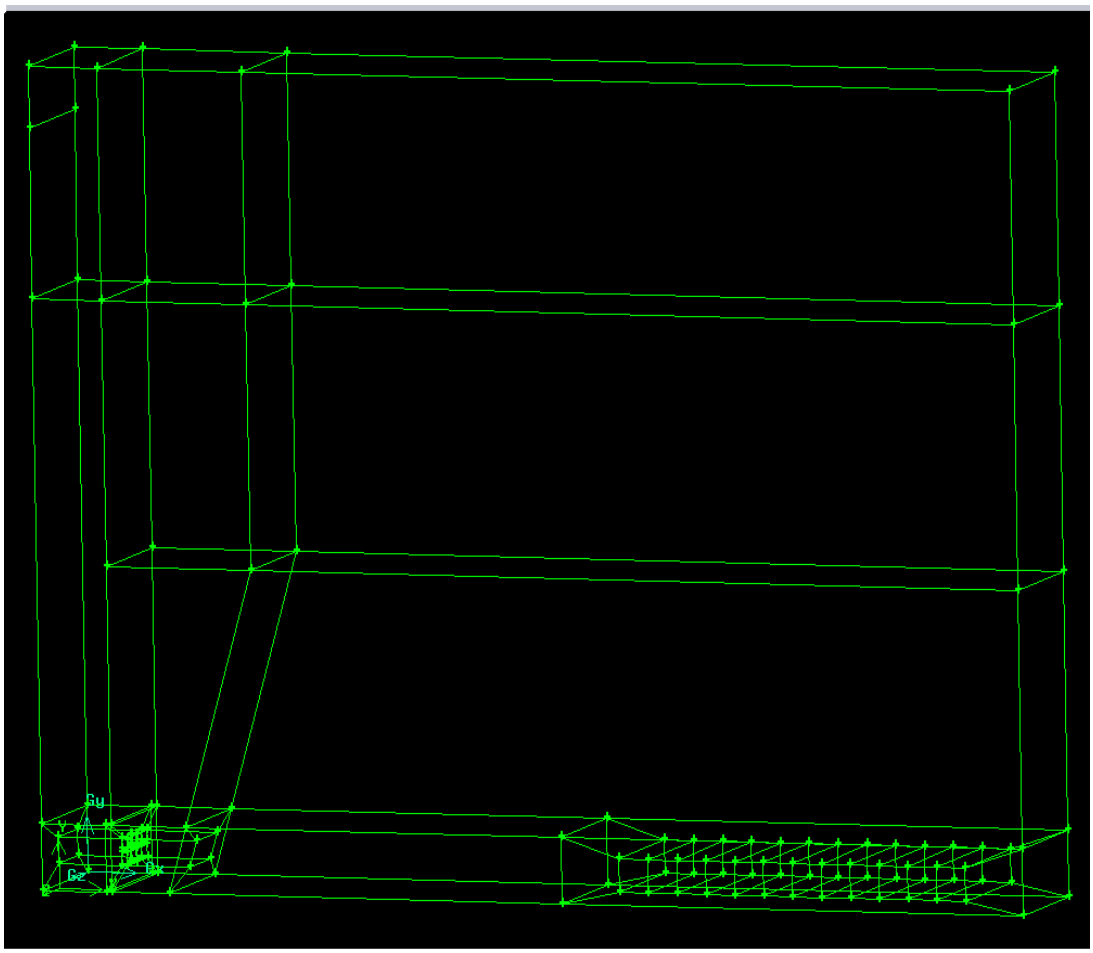

Figure 7. A schematic description of the three-dimensional thin strip (D) model including the inlet, contact and separation zone. One needle valve is modelled in the geometry.

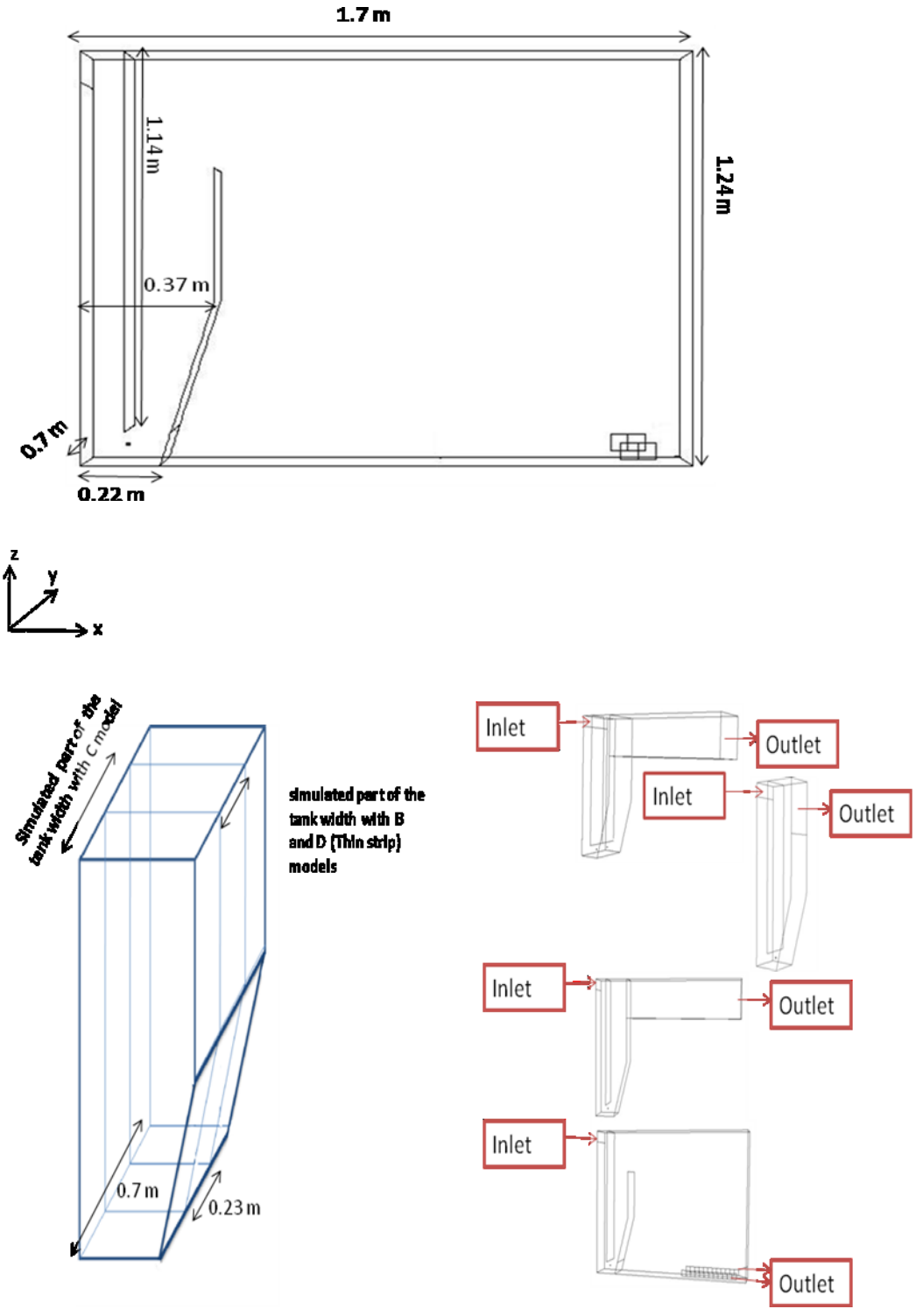

Figure 8. A schematic representation of the simulated tank geometry values and the simulated parts of the tank width through different models as well as location of the inlet and the outlet. The origin of the co-ordinate system is defined at the lower right corner of the tank.

3.1 Boundary condition

Boundary condition settings for velocity inlet includes: velocity magnitude, turbulence intensity and hydraulic diameter. For the pressure outlet turbulence intensity and hydraulic diameter are calculated. Table 1 shows design parameters used as boundary conditions in this study. The geometry values can be found in Figure 8 as well. The parameters are derived from experimental measurements done by Lundh (2000).

Parameter	Value	Parameter	Value
Top Length	0.37 m	**Baffle wall height**	1.14 m
Bottom Length	0.22 m	**Needle valve height**	0.005 m
Height	1.24 m	**Inlet velocity magnitude**	0.043 m/s
Width	0.23 m	**Needle valve velocity magnitude**	4.53 m/s
Inlet height	0.093 m	**Inlet and outlet turbulence intensity**	5.3 %
Outlet height (model A,B,C)	0.35 m	**Needle valve turbulent intensity**	6 %

Table 1. Design parameters used as boundary conditions in this study, are presented above. Turbulence intensity is calculated for both the velocity inlet and the outlet.

3.2 Solver settings and solution methods

Simple scheme is used as the solution method in this study. Spatial discretization scheme for momentum, turbulence kinetic energy and turbulence dissipation rate is set as second order upwind.

In this study a relaxation factor, α, which shows how much of old calculated values will be used to calculate new ones. In this study relaxation factor of 0.3 and 0.1 for the momentum and the turbulence respectively are found to improve convergence.

Part of the aim in this study is to examine how to model the needle valves in a complete model where both the contact zone and the separation zone are included. The turbulence kinetic energy is low and the flow is not affected by external forces, the flow is assumed to be in steady state (Bondelind, 2009).

Both the standard k- ε turbulence and the realizable k- ε model are evaluated in this study. Previous studies have shown that the standard k- ε model performs well for a one-phase flow, but the realizable model can improve the simulations for a two-phase flow (Bondelind et al. 2010)

The second phase, the air bubbles, is modelled with the Lagrangian model. Mono sized bubbles are used in this study. The parameters used to model the second phase are presented in Table 2. The injection location is at x=12 cm, y=1.15 cm and z=0.5 cm.

Parameter	Value
Injection location	x: 12 cm y: 1.15 cm z: 0.5 cm
Velocity	4.53 m/s
Bubble size	80 µm
Q_{rec}	$2.85*10^{-5}$ m/s
Number of air bubbles	32000

Table 2. Parameters used to model the second phase. Injection location values are regarding origin of the coordinate system presented in figure 8. All values are presented based on the three-dimensional model D.

3.3 Mesh dependence

Not having enough mesh cells reduces the accuracy of the results, but an unnecessarily large amount of cells will, on the other hand, increase the computation time. In order to find suitable number of mesh cells simulation is repeated with a refined mesh and if results are different, the refinement will be continued. In Table 3 the number of mesh cells used in this study is presented. Quadrangular elements are used and the mesh cells are smaller closer to the walls in order to account for wall effects.

Model	Number of cells
Two dimensions (A_1)	3048
Three dimensions (1/3 contact zone) (B_1)	78272
Thin strip	207680

Table 3. Number of mesh cells used in the models.

4 Results and discussions

In this section the numerical simulations are presented and validated with experimental measurements. Thereafter, a sensitivity analysis is presented.

4.1 Validation

In this part of the report numerical calculations of flow in the tank are presented and compared with experimental measurements made by Lundh (2000). The results are presented in two groups: one-phase flow (bubble free water) and the two-phase flow (water with bubbles). Moreover, the one-phase flow simulations are divided in two groups regarding the difference between results whether water is injected from the needle valves or not.

Numerical simulation results are presented at the same location as where the experimental measurements were made (Lundh, 2000). In Figure 9 (on the left hand side), five different lateral, vertical planes are shown in the model B_1. The results of the simulations will be presented at these sections in the contact zone. It has been discussed in Chapter 3 (Figure 8) that only a part of the whole tank width is simulated in this study. As a result of this, the results from numerical simulations can only be compared with the middle part of the presented experimental measurement. At the middle of Figure 9, two longitudinal, vertical planes are shown in model C_1, which are used to plot the flow pattern in contact zone and in the separation zone. At the right of the Figure 9, a sample of a lateral, vertical plane representing the whole tank geometry is showed, which is the same as the planes used to show the experimental measurement result, together with the parts of this plane that will be compared numerical simulation results.

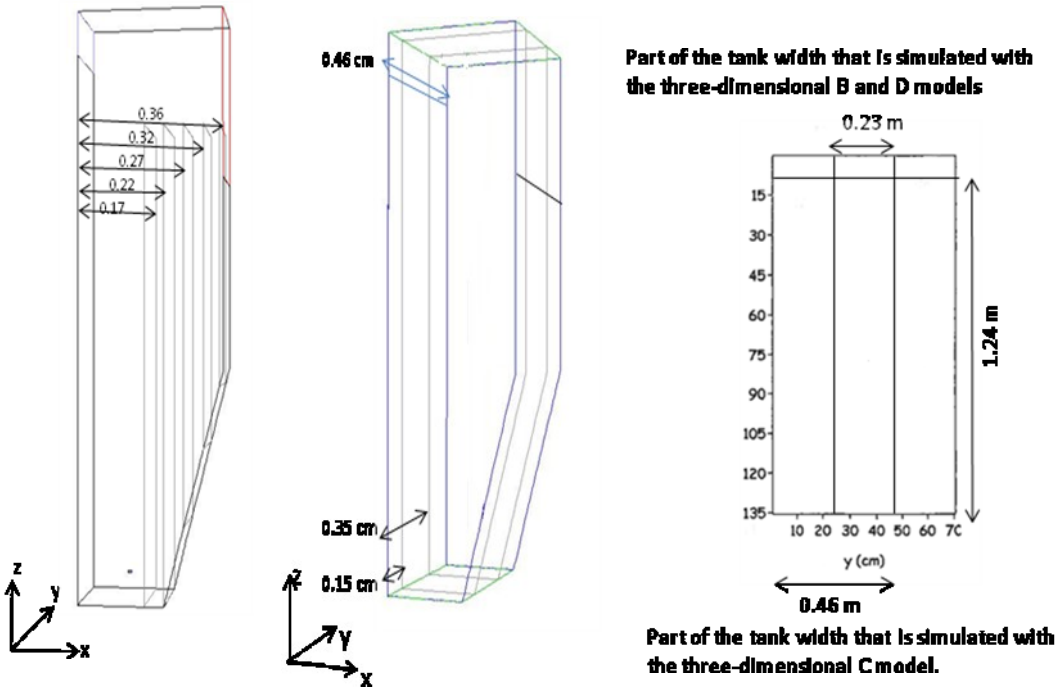

Figure 9. A schematic representation of the sections chosen in this study to show the simulated flow structure. The same locations are also used in the experimental study by Lundh (2000). The figure on the left shows five lateral vertical planes shown in the model B_1 and the figure in the middle shows two longitudinal, vertical planes shown in model C_1. The figure on the right shows part of the experimental measurement planes that can be compared with different model results.

Table 4 shows the general results in this study. The table shows which models reached convergence and which ones did not. Further in the report schematic representation of the flow pattern concluded from converged models will be discussed.

Model		Model name	Convergence		
			One-phase without injection of water from nozzle inlet	**One-phase with water injected from nozzle inlet**	**Two phase flow**
Without pipe	2D	(A_1)	No	-	No
	3D, Contact zone, 1 nozzle	(B_1)	Yes	Yes	No
	3D, Contact zone, 2 nozzles	(C_1)	No	No	-
With pipe	2D with pipe	(A_2)	Yes	Yes	No
	3D, Contact zone, 1 nozzle and a pipe	(B_2)	-	Yes	-
	3D, Contact zone, 2 nozzles and a pipe	(C_2)	-	Yes	-
3D, Thin strip		(D)	Yes	Yes	Yes

Table 4. The general results from all simulations that are carried out in this study. Dash lines show the simulations that are not performed in this study.

4.1.1 One-phase flow results (bubble free water)

4.1.1.1 Needle valves turned off

Results show that when there is no injection from needle valves simulation reaches to convergence without difficulties (without having inverse flow at the outlet). As it can be seen in Table 4, all models has converged solution when needle valves are turned off except two-dimensional A_1 model.

Figure 10 (Lundh, 2000), shows the flow pattern in the central, longitudinal, vertical section in contact zone. The flow pattern close to shaft wall is upward and it turns down ward close to the baffle. The largest velocities can be found close to the shaft wall and the maximum velocity is 7 cm/s.

Figure 11, shows the simulated flow pattern at the same section of contact zone for the two-dimensional A_2, three-dimensional B_1 and three-dimensional D models.

Numerical results are in accordance with experimental measurement. The upward flow pattern near the shaft and downward flow close to the baffle can be seen in all models.

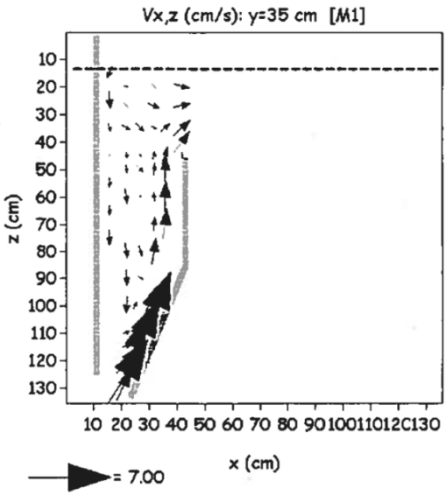

Figure 10. Experimental measurements of the flow pattern in longitudinal, vertical section in the contact zone in bubble free water and when the needle valves are turned off. (Lundh, 2000)

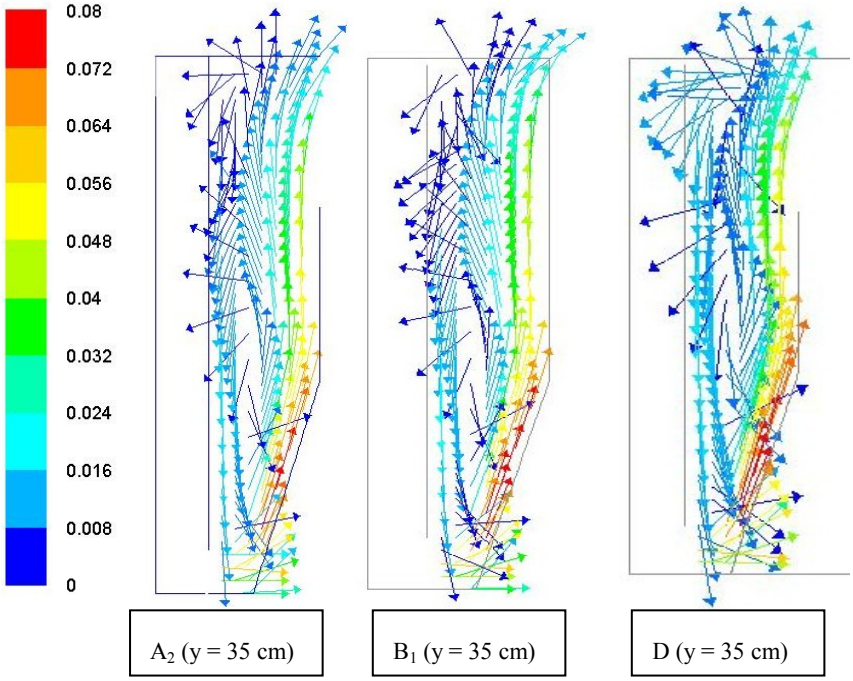

Figure 11. Numerical simulations of the flow pattern in central (y = 35 cm), longitudinal, vertical section in the contact zone in bubble free water and when needle valves are turned off. From left to the right; A_2, B_1 and D models are presented in sequence.

Moreover, three different lateral, vertical sections of these models are compared with experimental measurement results.

Figure 12, shows experimentally measured flow pattern (Lundh, 2000) in a vertical, lateral section of the contact zone. Results are plotted on a plane located at x = 22 cm. It should be noted that this plane shows the whole tank depth and width. The maximum velocity is 5 cm/s and larger velocity vectors are located at the bottom of the tank. Circulating patterns can be seen at the middle of the tank width. Central part of the tank width contains downwards flow structures.

Figure 13, shows numerical results plotted on the same plane and location as experimental measurements. It should be noted that these planes show the complete tank depth from the water surface to the bottom. But the plane only represents one third of the whole tank width. The three-dimensional models B_1 and D, from left to right in sequence, show the flow pattern in contact zone. The three-dimensional D model captures the downward movement observed in the experimental measurements, while the B_2 model predicts a flow patter moving upwards. Comparison of results with experimental measurements shows more similarities between the three-dimensional D model and the experimental results.

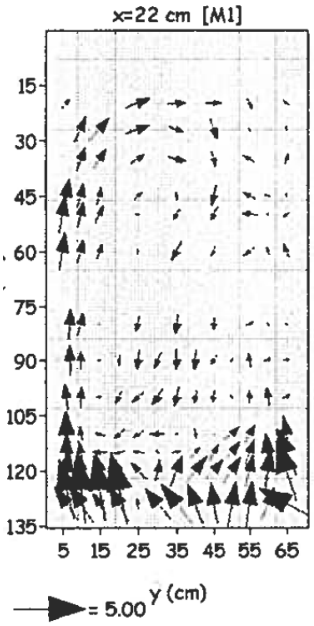

Figure 12. Experimental measurements of the flow pattern in vertical, lateral section in the contact zone in one phase flow and when there is no injection from needle valve (Lundh, 2000)

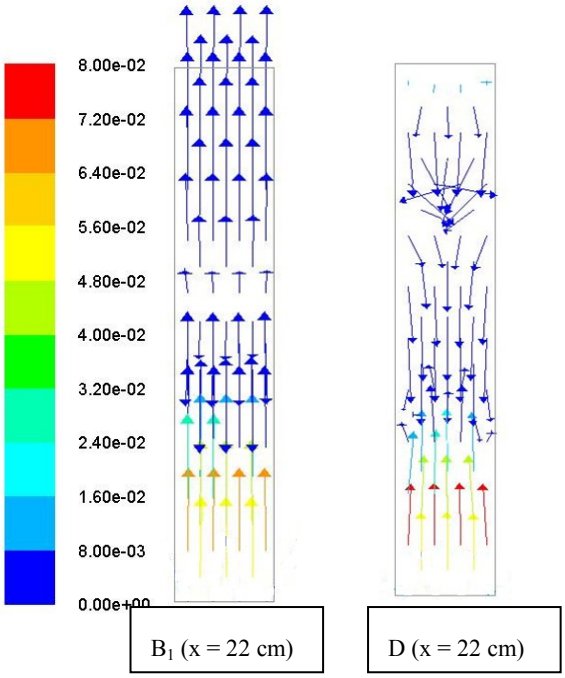

Figure 13. Numerical simulations of the flow in lateral, vertical section in the contact zone in bubble free water and when there is no water injection from the needle valve. Results are presented for the three-dimensional B_1 and D models from left to right in sequence, at x = 22 cm. Tank depth is up to the water surface (z = 124 cm) and one third of the whole tank width is simulated.

Two other sections examined are at x = 27 cm and x = 36 cm. According to Figure 14 (Lund, 2000) the maximum velocity is 8 cm/s at x = 27 cm and the largest velocity vectors appear at the bottom of the tank in this section. Circulating flow patterns can be seen in the middle of tank width in this plane. The largest velocity measured at x = 36 cm is 5 cm/s and the flow pattern is generally upward.

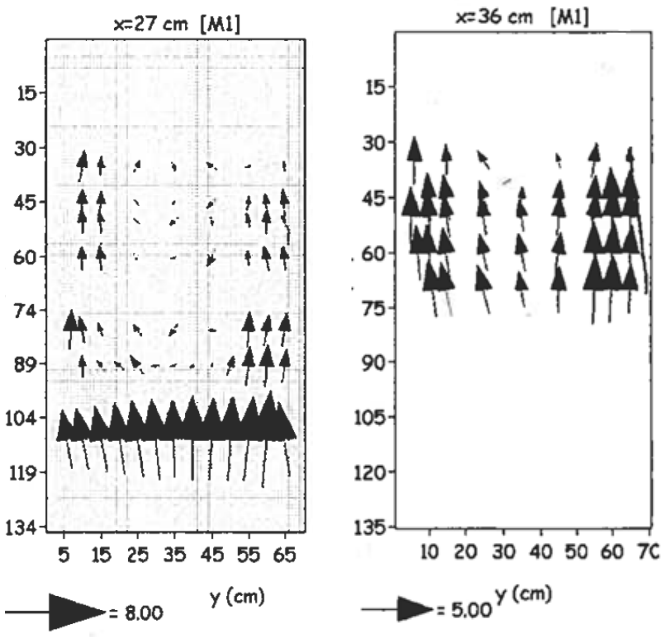

Figure 14. Experimental measurements of the flow pattern in vertical, lateral section in the contact zone in one phase flow and when there is no injection from needle valve (Lundh, 2000).

Figure 15, presents numerical results from the three-dimensional B_1 and D models at the planes x = 27 cm and x = 36 cm from left to right in sequence. As for the previous planes, the complete tank depth from the water surface to the tank bottom is shown and the reader is reminded that the planes only represents one third of the whole tank width. Both numerical models at these two sections show the same upward flow pattern.

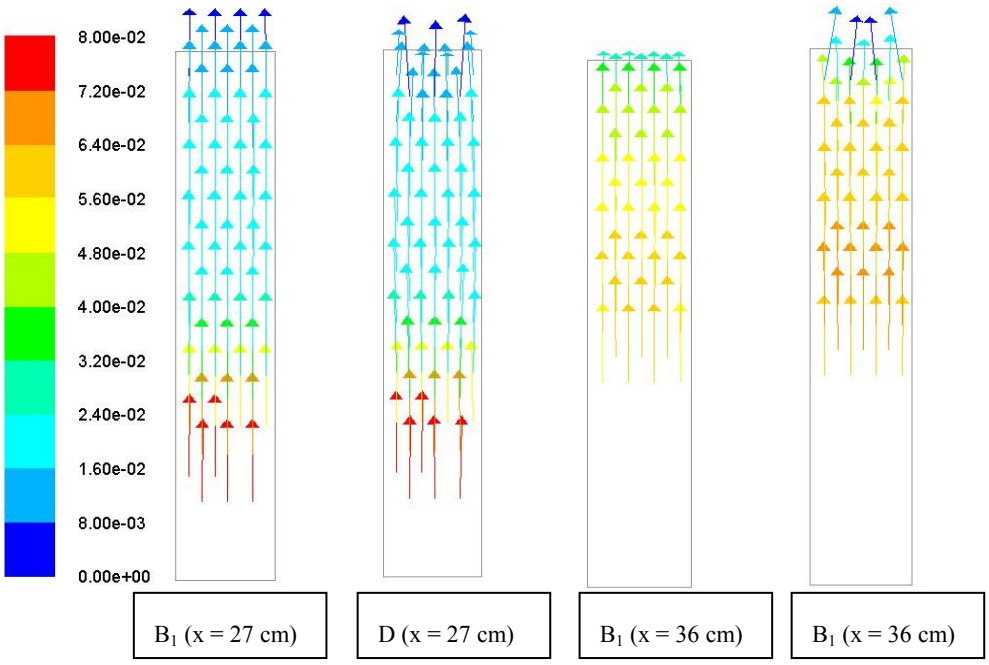

Figure 15. Numerical simulations of the flow in lateral, vertical section in the contact zone in bubble free water and when there is no water injection from needle valve inlet. Results are presented from the three-dimensional B_1 and D models, from left to right in sequence, and the flow pattern is plotted at the planes at x = 27 cm and x = 36 cm. The tank depth is shown from the water surface to the bottom and only one third of the whole tank width is simulated.

The flow pattern in the separation zone is simulated in the three-dimensional model D (*Thin strip model*). The flow structure in the longitudinal, lateral section of this model at y = 35 cm is presented in Figure 16, similarities in the flow pattern between simulations and measurements, Figure 17, can be found when comparing the results. However, there is there is a discrepancy in the velocity magnitude between simulations and experimental measurements. The maximum velocity magnitude concluded for the numerical simulations at this section is 4 cm/s, and 3 cm/s resulted for the experimental measurements.

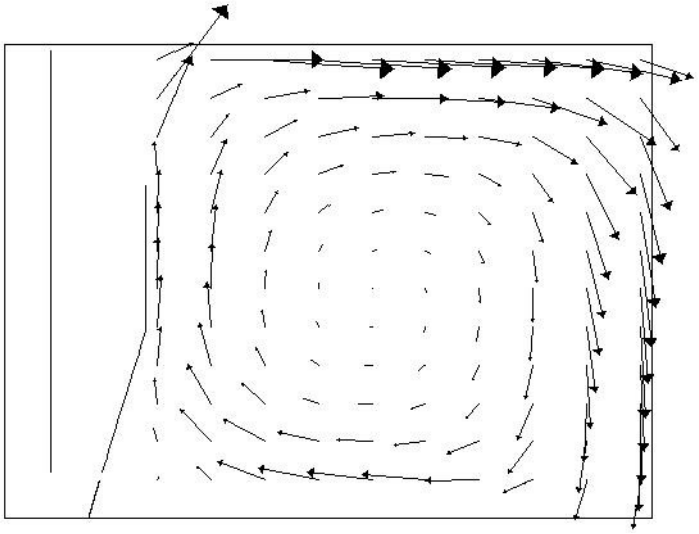

Figure 16. Simulated flow pattern in the central (y = 35 cm), longitudinal, vertical section of the three-dimensional model D in the contact zone and in bubble free water and when needle valves are turned off. Maximum velocity magnitude in this figure is 4 cm/s.

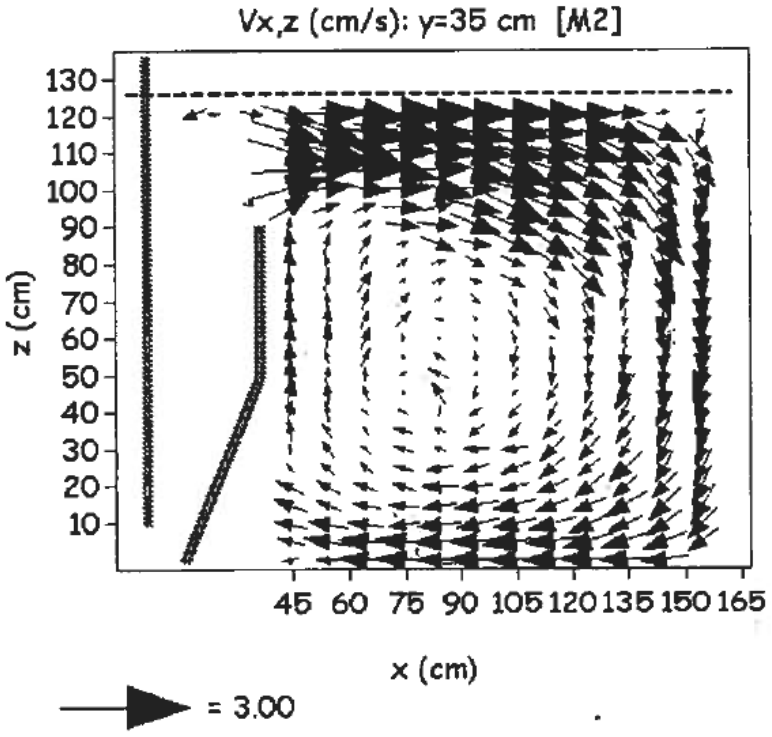

Figure 17. Experimentally measured flow pattern at a longitudinal, vertical section in the separation zone in bubble free water and when the needle valves are turned off (Lundh, 2000).

4.1.1.2 Needle valves turned on

Considerable changes happen in the flow structure when water is injected through the needle valves. Without inclusion of a long pipe at the outlet, reverse flow makes it difficult to reach a converged solution for some of the models.

Results at the central, longitudinal, vertical section in contact zone at y = 35 cm, for the three-dimensional B_1, C_2 and D models will be discussed first and compared with experimental measurements, Figure 18. The general experimentally determined flow pattern is directed upward, while some circulating water can be observed near the shaft wall and also close to water surface. The largest velocity is 10 cm/s, close to shaft wall. Figure 19, shows the simulated flow structure for the model B_1, C_2 and D. from left to right in sequence. General upward flow pattern as well as circulating flow structures near shaft wall and close to water surface exists in this model.

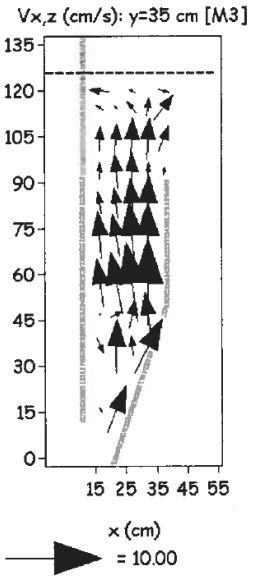

Figure 18. Experimental measurements of the flow pattern in longitudinal, vertical section in the contact zone in one phase flow and when needle valves are turned on (Lundh, 2000)

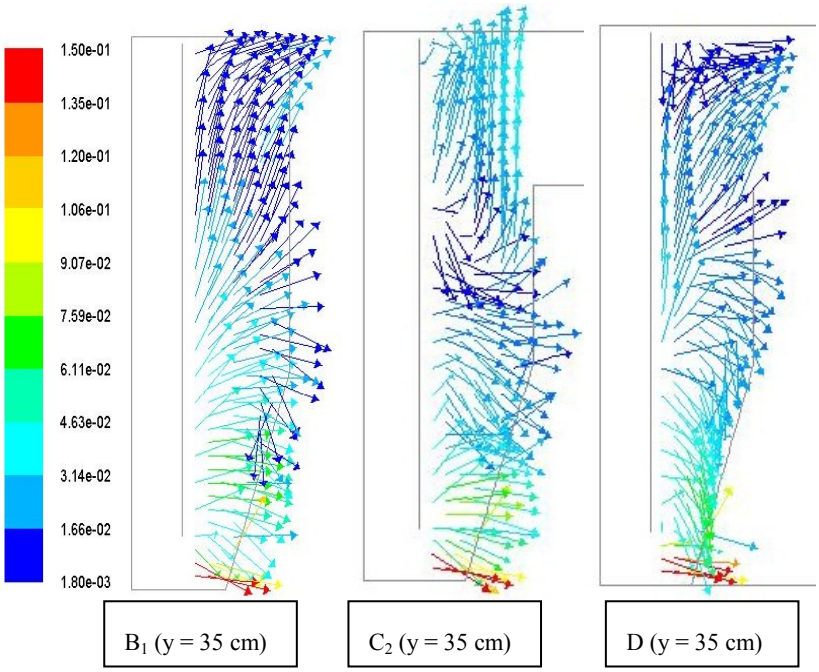

Figure 19. Numerical simulations of the flow pattern in central (y = 35 cm), longitudinal, vertical section in the contact zone in bubble free water and when needle valves are turned on. From left to the right B_1, C_2 and D models are presented in sequence.

Another longitudinal, vertical section of the three dimensional C_2 model at y = 15 cm is compared with experimental measurement results. Figure 20 shows the experimentally measured flow at the section y = 15 cm (Lundh, 2000). The flow pattern in this section contains circulating patterns close to the shaft wall and the flow is directed upward at the upper parts of the contact zone. Higher velocities can be seen near the shaft and the maximum velocity is 4 cm/s. Similarities in the flow pattern is observed when the experimentally determined flow pattern is compared with the simulated flow pattern for model C_2, Figure 21.

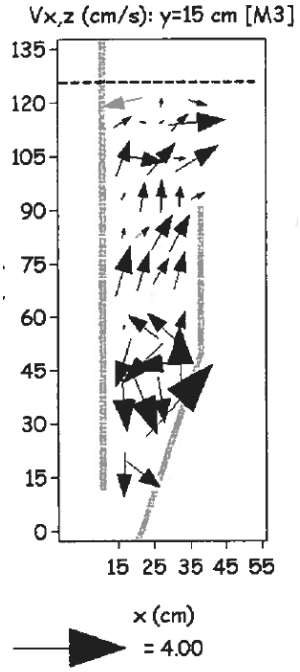

Figure 20. Experimental measurements of the flow pattern at the longitudinal, vertical section in the contact zone in one phase flow and when the needle valves are turned on (Lundh, 2000)

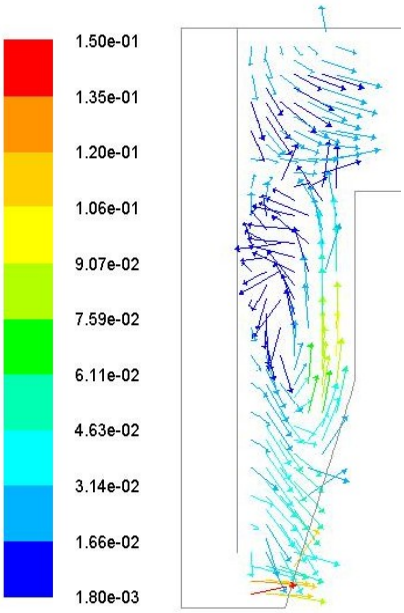

Figure 21. Numerical simulations of the flow pattern at the central longitudinal, vertical section in the contact zone at y=15 cm for the three-dimensional C_2 model, in bubble free water and when needle valves are turned on.

Results from the three dimensional models B_1, C_2 and D at x = 17, 27 and 32 cm are compared with experimental measurements. Figure 22 (Lundh, 2000) shows experimental measurement results in lateral, vertical section in the contact zone at x = 17, 27 and 32 cm from left to right in sequence. General flow pattern at the middle of all sections is directed upward and circulating patterns can be seen at sides. Maximum velocity is 6 cm/s at x = 17 cm, 9 cm/s at x = 27 cm and 10 cm/s at x = 32 cm, which happens at the middle of these sections.

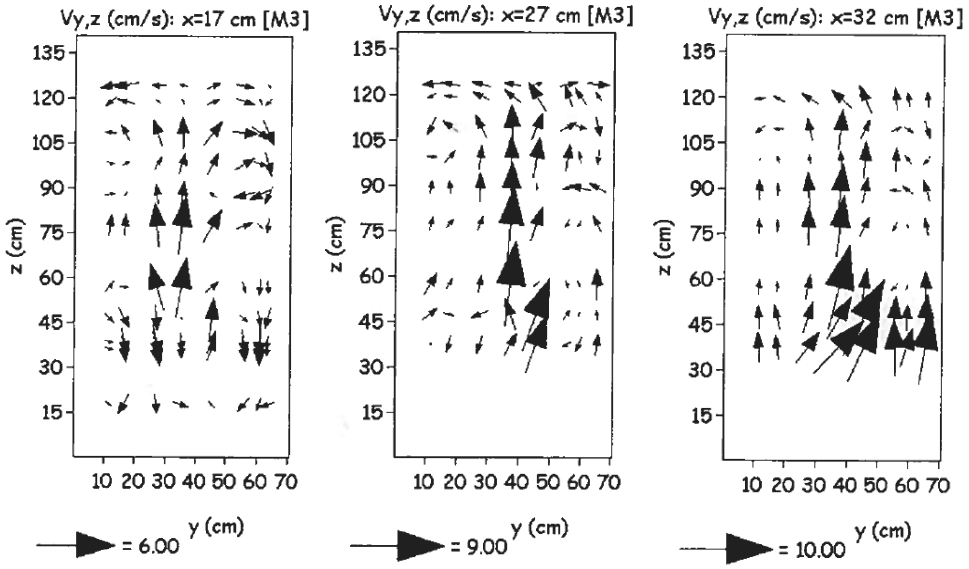

Figure 22. Experimental measurements of the flow in the lateral, vertical section in the contact zone in bubble free water and when needle valves are turned on (Lundh, 2000)

The simulated flow pattern for the three-dimensional B_1 model is shown in Figure 23. General upward flow pattern and also circulating pattern at the bottom can be seen at all sections. Circulating structures reduces close to the shaft wall.

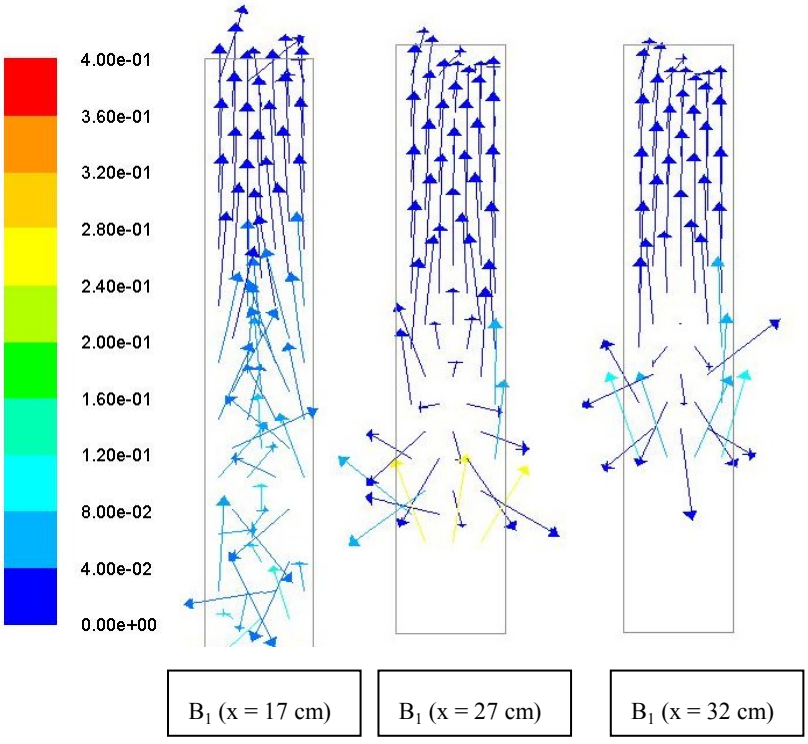

Figure 23. Numerical simulations in the lateral, vertical section of the contact zone in bubble free water and when needle valves are turned on. Results are presented in accordance to three-dimensional B_1 model at x =17, 27 and 32 cm from left to right in sequence. Tank depth is up to the water surface (z = 124 cm) and only one third of the tank width is simulated.

Velocity vectors at the same sections are also plotted for the three-dimensional C_2 and D models, Figure 24. The first row represents the C_2 model and in the second row simulated results from model D are presented. Each row contains lateral, vertical sections in the contact zone at x = 17, 27 and 32 cm from left to right in sequence. Circulating patterns at the top of the figures concluded from three-dimensional C_2 model shows obvious circulating patterns at bottom and the top, which is very similar to experimental results. The general flow pattern in both models is upward, which is in accordance with measurement results.

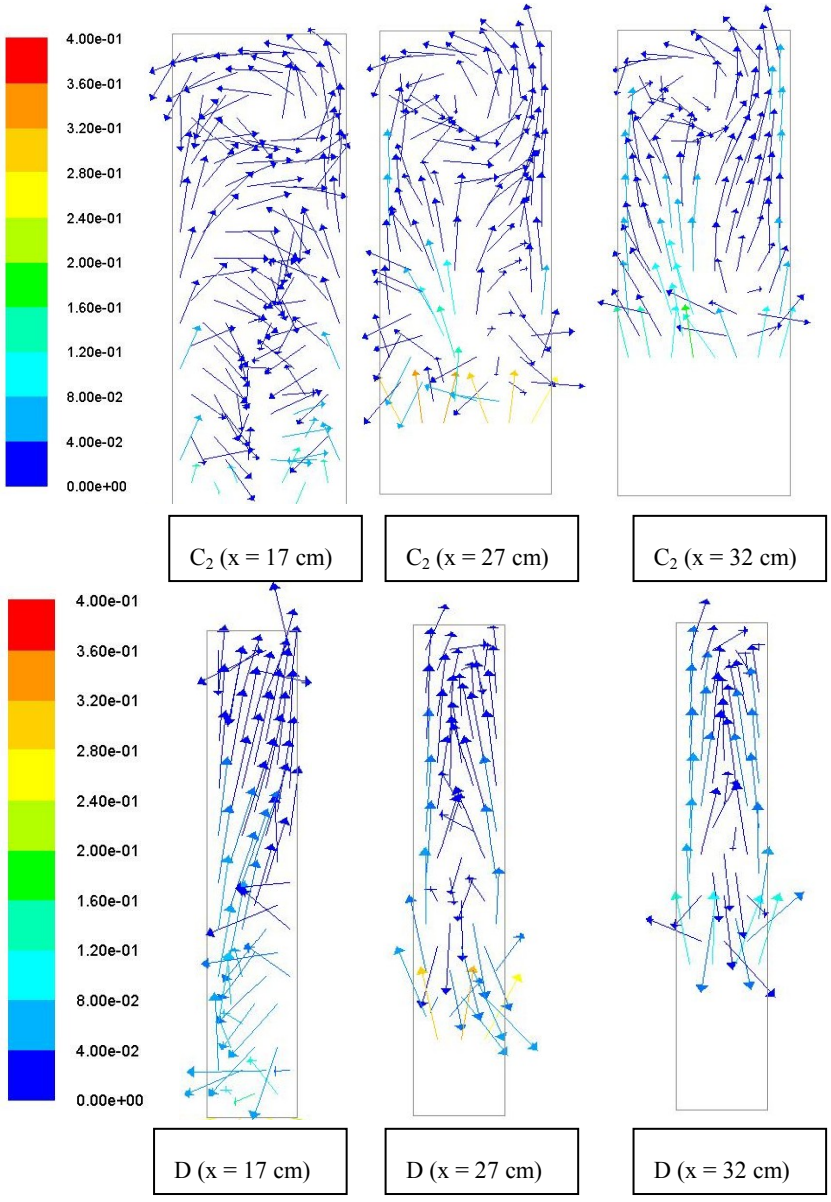

Figure 24. Numerical simulations in lateral, vertical sections in the contact zone in bubble free water and when needle valves are turned on. Results are presented in accordance to three-dimensional C_2 (first row) and D (second row) models. Each row presents flow structures at x = 17, 27 and 32 cm from left to right in sequence. Tank depth is up to the water surface (z = 124 cm).

In order to validate accuracy of the three-dimensional model D (Thin strip model), the flow structure in longitudinal vertical section of the separation zone at y = 35 cm,

Figure 25, is compared with experimental measurement results, Figure 26. Similarities between simulated and experimental flow structure in this section are observed. The maximum velocity magnitude obtained from the simulation is around 4 cm/s, which is the same as for the experimental measurements.

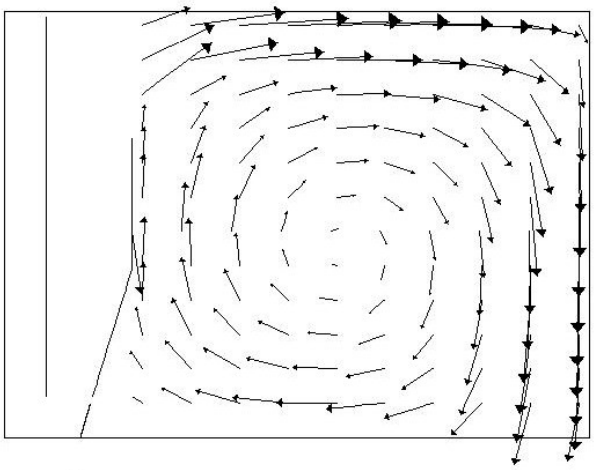

Figure 25. Numerical simulations in the central (y = 35 cm), longitudinal, vertical section of the three-dimensional model D in the contact zone in bubble free water and when needle valves are turned on. The maximum velocity magnitude seen in the figure is 4 cm/s.

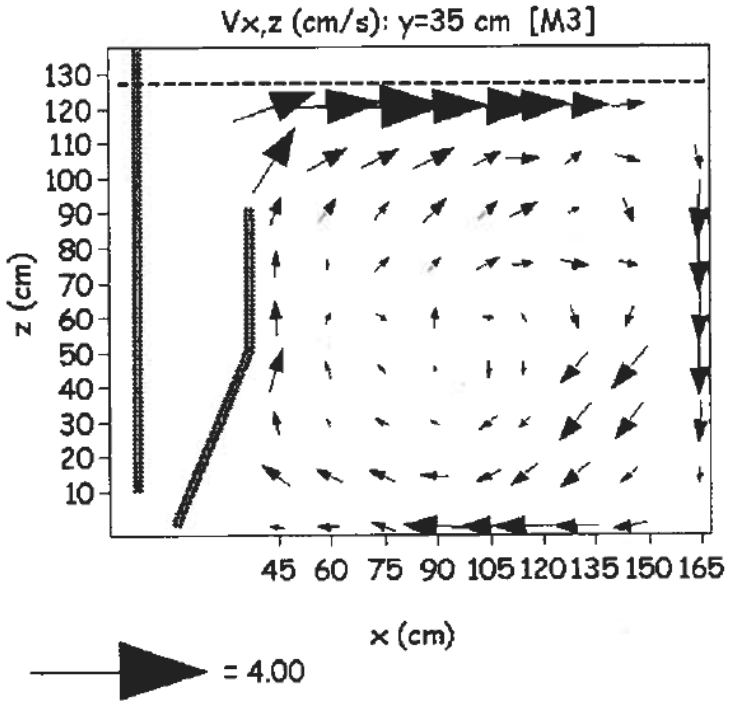

Figure 26. The experimental measurements of the flow pattern in central (y = 35 cm), longitudinal, vertical section of the three-dimensional model D in the contact zone in bubble free water and when needle valves are turned on (Lundh, 2000).

4.1.2 Two-phase flow results (water with bubbles)

Two-phase simulations are preformed for two- and three-dimensional models. The computational time and space needed for these simulations is very demanding. Also convergence cannot be reached very easily for a steady state solution and therefore it is recommended to try transient solver in future studies. The only model for which a converged solution can be found is the *Thin strip model*. The simulated flow in the three-dimensional model D, Figure 28, is compared with experimental measurement results, Figure 27, and some similarities are found.

Considerable differences are found when the simulated two-phase flow is compared with the one-phase flow, Figure 19.

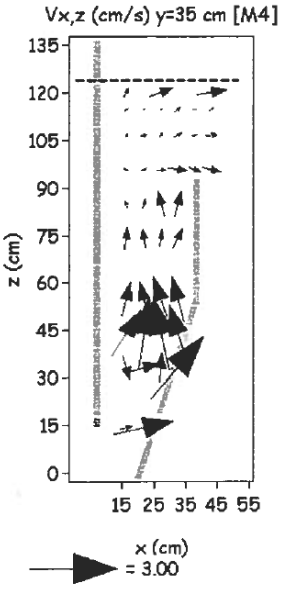

Figure 27. Experimental measurements of the flow pattern in longitudinal, vertical section in the contact zone for a two-phase flow. (Lundh, 2000)

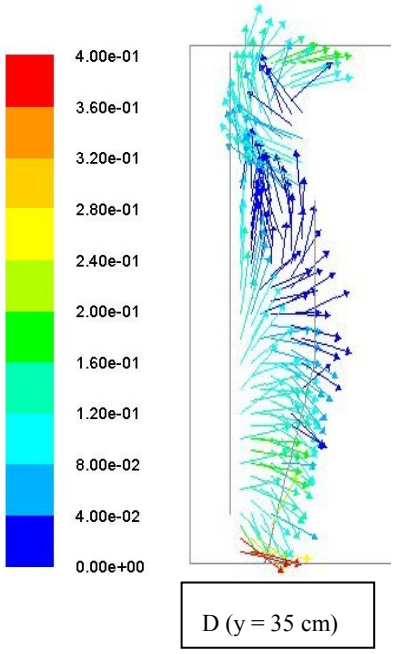

Figure 28. Numerical simulations in central longitudinal, vertical section in the contact zone at y = 35 cm concluded from three-dimensional D model, for a two-phase flow.

Figure 29 shows experimental measurements at three different lateral, vertical planes in contact zone and Figure 30 presents the numerical simulations for the same sections. These planes are located at x = 17, 27 and 32 cm, in both figures from left to right in sequence. Upward flow direction at the middle of all the planes in Figure 29 and some circulating patterns can be seen in Figure 30.

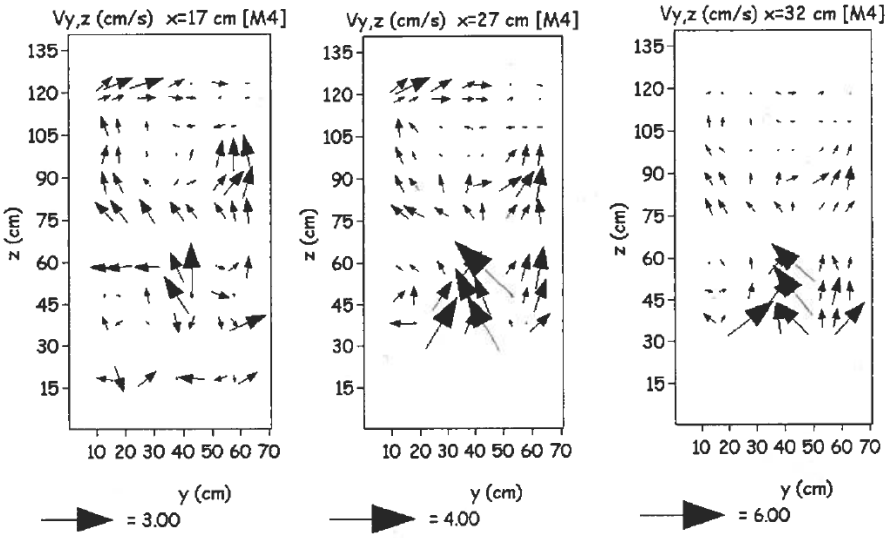

Figure 29. Experimental measurements of the flow pattern in lateral, vertical section in the contact zone for a two phase flow. (Lundh, 2000)

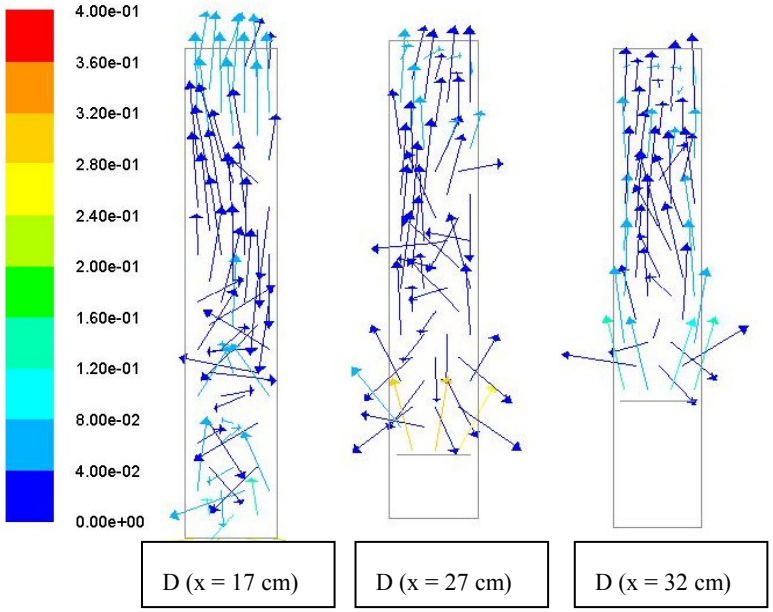

Figure 30. Numerical simulations in lateral, vertical sections in the contact zone for a two phase flow, concluded from the three-dimensional model D. Plotted sections are located at x =17, 27 and 32 cm from left to right in sequence.

Flow pattern in separation zone is also compared with experimental measurement results. Figure 31, shows the flow pattern at longitudinal, vertical section of the separation zone. Higher velocities can be seen close to the water surface and the maximum detected velocity is 1.5 cm/s. The simulated two-phase flow structure at the same longitudinal section in separation zone is presented in Figure 32. The larger discrepancies in flow structure observed between simulated and experimentally measured flow in the separation zone for a two-phase flow, compared to a one-phase flow, should be further evaluated. The higher magnitude of the velocities detected in the simulations (7 cm/s) compared to the experimentally determined velocity (1.5 cm/s) are considered to be caused by the measuring equipment used when performing the measurements. The air bubbles disturbed the ADV probe while measurements where performed and the measured velocity magnitude was reduced.

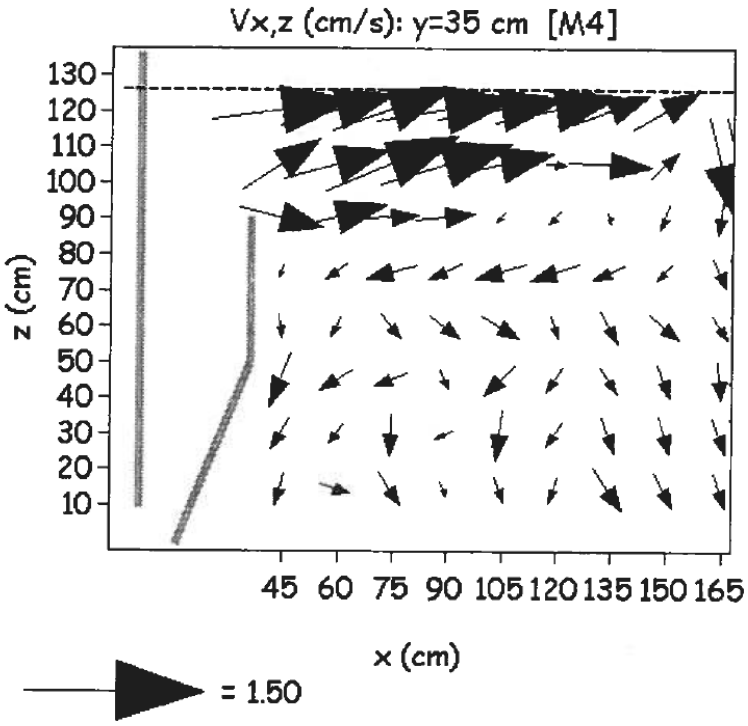

Figur 31. Experimental measurements of the flow pattern in longitudinal, vertical section in the seperation zone for a two-phase flow (Lundh, 2000).

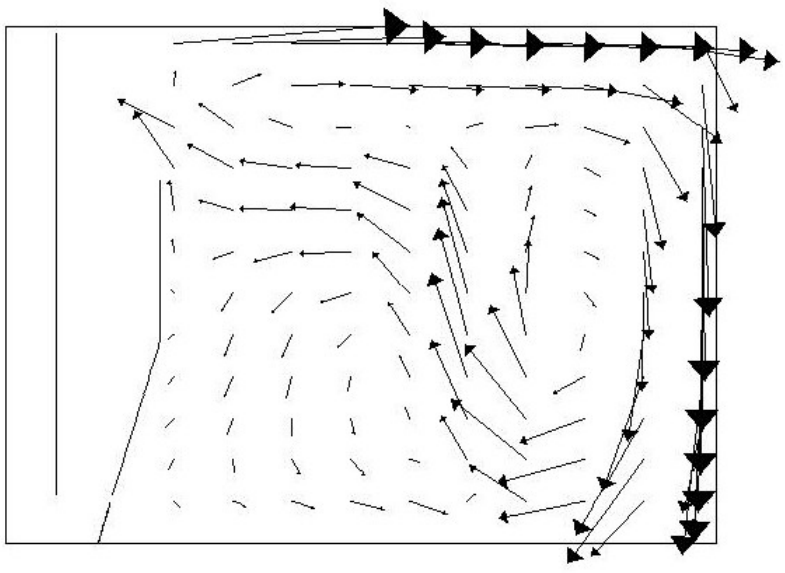

Figur 32. Numerical simulations of the flow pattern in the central longitudinal, vertical section in the separation zone at y = 35 cm for the three-dimensional, two-phase D model.

The concentration of air bubbles is another way of presenting results for a two-phase flow. The concentration of the second phase in the three-dimensional model D in the longitudinal, vertical section of the tank at y = 35 cm, is presented in Figure 33. The model predicts that a small concentration of air bubbles escaping in to the inlet zone, a phenomenon not observed in the experimental measurements. The air distribution and

the flow structure are closely linked together and the escape of the air bubbles can perhaps be related to the fact that the flow structure in the simulated separation zone has not been produced well enough.

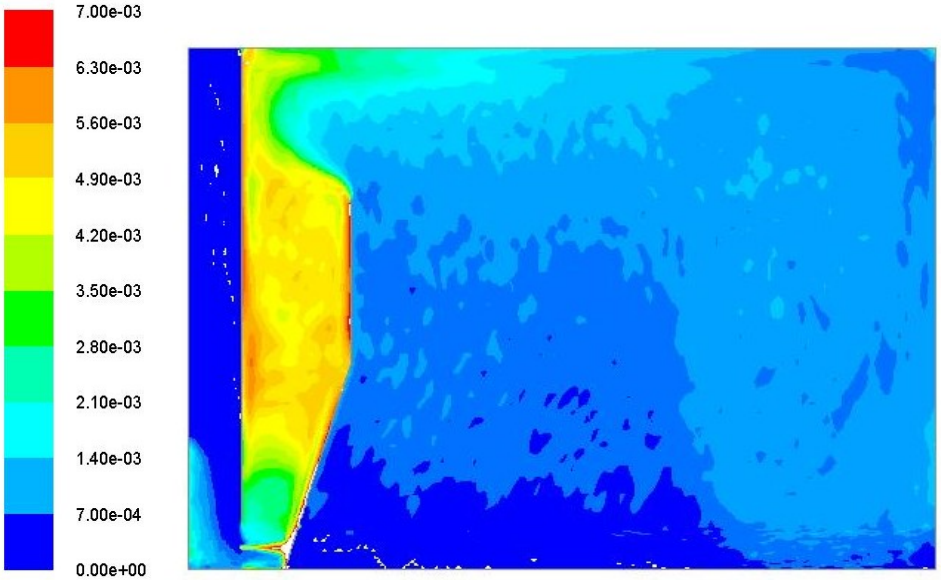

Figure 33. A schematic presentation of air concentration concluded from three-dimensional model D plotted in the longitudinal, vertical section of the tank at y= 35 cm.

4.2 Evaluation of the numerical models

This chapter addresses a sensitivity analysis of the effects of different parameters on flow structure in contact zone. This analysis is only carried out for the one-phase flow simulations.

It has been discussed in Chapter 3 and at the beginning of Chapter 4, that because of difficulties to reach convergence for two-dimensional model A_1 and three-dimensional model B_1 and C_1, an extended outlet has been designed, which lead to two-dimensional model A_2 and three-dimensional model B_2 and C_2. Model B_1 is the only model, which can reach to convergence without need to have an extended outlet, Table 4, so flow structure in this model is compared with model B_2 in order to check effects of the extended outlet on flow pattern in contact zone. Results show that there is not any considerable difference in these two models flow structures, when the needle valves are turned off, while when the needle valves are turned on, there are considerable differences between flow patterns of these two models. Flow structure in longitudinal, vertical section of contact zone of three-dimensional model B_2 is presented in Figure 34. Comparing this with Figure 19, which shows flow structure of three-dimensional B_1, C_2 and D model, it can be seen that there are similarities between flow structure of model B_2 and D.

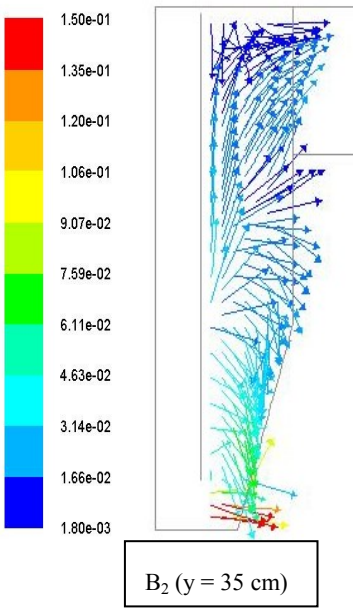

Figure 34. Numerical simulations of the flow pattern in central longitudinal, vertical section in the contact zone at y = 35 cm concluded from three-dimensional B_2 model, in bubble free water and when needle valves are turned on.

Moreover, the differences between the standard k-ε turbulence model and the realizable k-ε turbulence model are evaluated. Results show that when there is no flow injected from the needle valves, there is not any difference between these two models. However, when the needle valves are turned on, small differences exists between the different models. Figure 35, shows the flow structure with the same characteristics as Figure 34, but only with the difference of using standard k-ε turbulence model. By comparing these two figures differences in flow pattern can be observed. It should be noted that all the previous figures at the validation chapter are simulated based on the realizable k-ε turbulence model in order to make sure that the differences between these two models will not affect the validation.

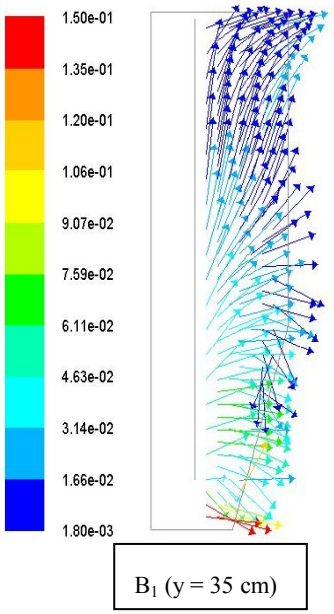

Figure 35. Numerical simulations of the flow pattern in central longitudinal, vertical section in the contact zone at y = 35 cm concluded from three-dimensional B_1 model, in bubble free water and when needle valves are turned on and with standard k-ε turbulence model.

The side walls are considered as symmetric walls because of the location of simulated part of the tank, Figure 9, which is at the middle part of the tank. In order to study sensitivity of flow structure on this matter, model C_2 is changed to have a non-symmetric front wall. Results are presented in the longitudinal, vertical section of this model at y = 15 cm, Figure 36. Comparing Figure 36 with Figure 21, which presents the flow structure at the same section of the same model and with two symmetric side walls, it can be observed that differences in the flow pattern exists.

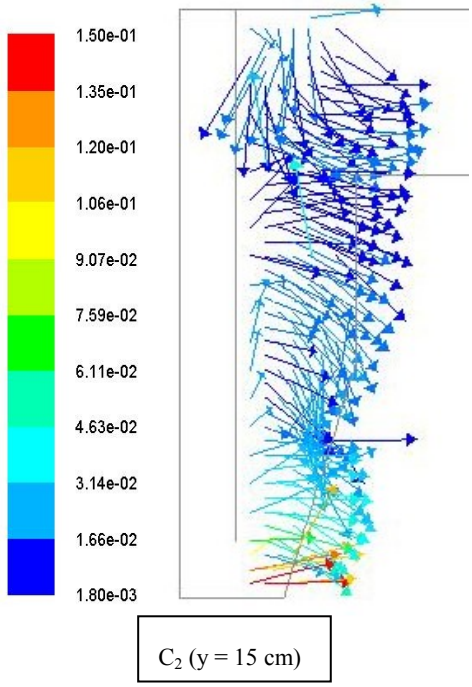

Figure 36. Numerical simulations of the flow pattern at the longitudinal, vertical section in the contact zone at y = 15 cm for the three-dimensional C_2 model, in bubble free water and when the flow from the needle valves are turned on.

Also, different outlet locations for the three-dimensional model D (Thin strip), is examined and the results shows that no considerable difference is evident. Different outlet locations are accounted for as of being different combinations of two outlet boxes (Figure 8) on each side wall.

4.3 Concluding Discussion

Comparing the simulated flow structure in different sections of the tank shows that although similarities can be observed in one section, but differences in the flow pattern in other sections exists. For example Figure 11, shows very close similarities between the two-dimensional model A_2 and the three-dimensional model B_1 and model D, in central, longitudinal, vertical section, while considerable differences can be detected in lateral, vertical sections, Figure 13, 15.

Two-dimensional model shows good accuracy when the effects of injection of water from needle valves is excluded. However, when the needle valves are turned on a two-dimensional model cannot capture the flow pattern. Neither can a two-dimensional model account for the effects of side walls. Therefore this model is not recommended to be used to model the contact zone.

It is said before in Chapter 3, that the reason for considering the flow field to be in steady state is that no external forces exists and turbulent kinetic energy is low. Although this matter is more accurate in separation zone, but considering that evaluation of contact zone in steady state has not been tried before, and the fact that modeling separation zone together with contact zone is considered in the scope of the project, it has been decided to assume steady sate flow field in this study. It should be noted that steady state solution requires less computational time than a time dependent solution.

Moreover, less computational time is required for calculating steady state flow and also considering a model for both contact zone and separation zone (full tank) are the other reasons of this selection.

The three-dimensional model C shows considerable similarities with experimental measurements especially the circulating flow patterns in different sections of the contact zone. But reaching the convergence with this model is much harder comparing to other models. The reason of this matter could be because of the effects of two needle valves in this model. Thinking about a transient solver might improve difficulties to reach convergence.

5 Conclusions

Three different representations of the contact zone have been evaluated in this study. A two-dimensional model, a three-dimensional model considering one third of the tank width with one needle valve and a three-dimensional model representing two thirds of the tank width with two needle valves. Simulations have been carried out for both one- and two-phase flows.

It is concluded that the one-phase flow in the contact zone can to some extent be modelled with a two-dimensional model if no water is injected from the needle valves. However, if the flow from the needle valves is turned on a three-dimensional model should be used.

Identified parameters having an effect on the flow structure in a three-dimensional model are:

- The results show that the flow from the needle valves will interact causing a complex flow structure in the contact zone. The number of needle valves included in a model should therefore be considered when setting up a numerical model.
- The choice of a symmetric or a non symmetric side wall will influence the flow.
- Modelled outlet geometries for the contact zone affect numerical convergence. Having an outlet very close to the contact zone leads to a reverse flow at the outlet. It is also observed that the flow pattern is influenced by the inclusion of the separation zone.
- The choice of turbulence model should be considered when setting up a numerical model of the contact zone.
- The addition of the second phase affects the flow pattern to a large extent. Difficulties finding a converged solution for the evaluated models suggest that possibly a transient solver should be used if the flow in the contact zone is to be resolved.

5.1 Future work

Recommendations for a future work in this area are:

- Considering a time dependent solution for the flow structure in the contact zone.
- Further investigation on the reasons of finding backward movement of air bubbles in to the inlet zone.
- Evaluating other ways of modelling the outlets. For example using a coarser mesh in the separation zone, while the mesh in contact zone is fine enough in order to account for the effects of the separation zone and reduce the computation time.

6 References

ANSYS. (2010, June). Retrieved from http://www.ansys.com

Batchelor, G. K. (1967). An Introduction to Fluid Dynamics . Cambridge univsity press.

Bondelind, M. (2009). Numerical Modelling of Dissolved Air Flotation . Gothenburg, Sweden : Chalmers University of Technology.

Bondelind, M. Sasic, S. Pettersson, T.J.R. Karapantsios, T.D. Kostoglou, M. Bargdahl, L. (2010). Setting up a numerical model of a DAF tank: Aspects on turbulence, geometry and bubble size, In press, J. Env. Eng.

Crossley, I. A. Rokjer, D and Kim, J. (1999). Optimization the DAF process utilizing two-phase3D CFD modelling. Proc. AWWA Chicago, Illinois, Vol 43 No 8 pp 35-42.

Date, A. W. (2005). Introduction to Computational Fluid Dynamics. Cambridge university press.

Davidson, L. (1997). An Introduction to Turbulence Models. Gothenburg: Dept. of Thermo and Fluid Dynamics, Chalmers University of Technology.

Emmanouil, V. Skaperdas, E. P. Karapantsios, T. D and Matis. K. A. (2007). Two-phasesimulations of an off-nominally operating dissolevd air flotation tank . Environment and Pollution , Vol. 30, No. 2.

Guimet, V. Broutin, C. Vion, P and Glucina. K. (2007). CFD Modeling of high rate Dissolved Air Flotation . 5th International Conference on Flotation in Water and Wastewater. Seoul, South Korea.

Fawcett, N.S.J. (1997). The hydraulics of flotation tanks: computational modeling. Dissolved Air Flotation , Proc. Int. Conf. Chartered Institute of Water and Environmental Management, London, Pages 51-71.

Fluent. (2006). Fluent 6.3 users guide. Fluent Inc., 10 Cavendish Court, Lebanon, NH, USA.

Hague, J. Ta, C.T and Biggs, MJ. (2001a). Dense Micro-Bubble flow system CDF modeling and experimental validation. Proc. International Conference Multiphase Flow ICMF, Hague.

Lundh, M. (2000). Flow structures in Dissolved Air Flotation . Licentiate thesis, Lund University, Lund Sweden.

Lundh, M. (2002). Effects of flow structure on particle seperation in Dissolved Air Flotation . PhD thesis, Lund University, Lund Sweden.

Kown, S. B. Park, N. S. Ahn, S. J. and Wang, C. K. (2006). Examining the effect of lengh/ width ratio on the hydro dynamic behaviour in a DAF system using CFD and AVD techniques. Water Science and Technology, Vol 53 No 7 pp 141-149.

Ta, C. T and Brignal, W. J. (1997). Application of single phase Computational Fluid Dynamics techniques to Dissolved Air Flotation studies. Dissolved Air Flotation , Proc. Int. Conf. Charterd institute of Water and Environmnetal managemnet, London, pages 471-487.

Ta, C. T. Beckley, J and Eades, A. (2001). A multiphase CFD model of DAF process. Water Science and Technology, Vol 43 No 8 pp 153-157.

Tchobanoglous, G, Burton, F. L, and Stensel, H. D, Inc Metcalf & Eddy. (2003). Waste Water Engineering. McGraw-Hill.

Warren Viessman, M. J. (2005). Water Supply and Pollution control . Pearson Prentice Hall.

White, F. M. (2003). Fluid mechanics fifth edition . McGraw-Hills Companies.